COMPENSATION AND SIGNAL CONDITIONING OF CAPACITIVE PRESSURE SENSORS

Matej Možek, Danilo Vrtačnik, Drago Resnik, Borut Pečar, Slavko Amon

Laboratory of Microsensor Structures and Electronics (LMSE), Faculty of Electrical Engineering, University of Ljubljana, Ljubljana, Slovenia

Key words: digital temperature compensation, Chisholm approximation, Padé approximation, capacitance to digital converter.

Abstract: Implementation of a novel digital temperature compensation method, developed for piezoresistive pressure sensors, to the field of capacitive sensors is presented. Possibilities for the compensation of sensor parameters such as sensor nonlinearity and temperature sensitivity are analyzed. In order to achieve effective compensation and linearization, different approaches to digital descriptions of sensor characteristic are investigated and reported, such as two-dimensional rational polynomial description and Chisholm approximants. Results of sensor response are compared against reference pressure source and most effective digital temperature compensation is proposed.

Kompenzacija in obdelava signalov kapacitivnih senzorjev tlaka

Kjučne besede: digitalna temperaturna kompenzacija, Chisholm−ova aproksimacija, Padé−jeva aproksimacija, kapacitivno−digitalni pretvornik

Izvleček: V prispevku je predstavljene aplikacija metod digitalnih temperaturnih kompenzacij s področja piezorezistivnih senzorjev tlaka na področje kapacitivnih senzorjev tlaka. Analizirane so možnosti kompenzacije senzorskih parametrov kot sta nelinearnost in temperaturna občutljivost. Opisani so različni pristopi k digitalnemu opisu senzorske karakteristike, dvodimenzionalna polinomska aproksimacija in Chisholmovi aproksimanti. Rezultati kompenziranega senzorskega odziva so primerjani z referenčnimi meritvami tlaka. Na osnovi izmerjenih rezultatov je predlagana najbolj učinkovita metoda digitalne temperaturne kompenzacije kapacitivnih senzorjev tlaka.

1. Introduction

Sensors that exhibit a change in electrical capacitance as a response to a change in physical stimulus represent an attractive approach for use in modern sensor systems due to their extensive range of applications such as humidity, pressure, position sensors etc. Their broader range of applications include biomedical, touch & non-touch switch technology, proximity sensing, fingerprinting, automotive applications, robotics, materials property, and applications in motion sensors. This versatile sensor category offers higher precision and robustness, simpler construction and lower power consumption than resistive-based alternatives. However, they traditionally require more complex interfacing circuits, which represented a major disadvantage in the past. In a capacitive sensor, the physical parameter being measured by varying one or more of the quantities in the basic equation of capacitance

$$C = \varepsilon \frac{A}{d} \qquad (1)$$

where ε is the permittivity of the dielectric, A is the overlap area of the capacitor plates, and d is the distance between the plates. For example, humidity sensors typically work by varying the permittivity ε, pressure sensors by varying distance d and position sensors by varying area A or distance d. Measurement of the sensor capacitance is generally achieved by applying an excitation source to the capacitor electrodes which is used to turn variance in capacitance into a variance in voltage, current, frequency or pulse width

variation. Translation from voltage or current to a digital word requires an additional analog to digital converter (ADC).

The expected variance in capacitance is generally in the order of several pF or less. In many cases the stimulus capacitance change is much smaller than the parasitic capacitances present in the measuring circuit, hence representing a difficult interfacing task. However, a modification of conventional sigma−delta analog to digital converter architecture has been identified as a suitable basis for monolithic Capacitance to Digital Converter (CDC) /1/. Circuit itself is parasitic insensitive, and can be configured to work with both floating (access to both sensor terminals) and grounded configuration sensors (one terminal grounded).

Precision capacitive sensor interface products are based on a well established sigma-delta ($\Sigma\Delta$) conversion technology. Converters utilizing $\Sigma\Delta$ principle offer excellent linearity and resolution and are appropriate for most sensor interfacing applications. A typical $\Sigma\Delta$ converter ADC consists of switched-capacitor modulator followed by a digital filter. The modulator operation is based on balancing, over time, an unknown charge with a known reference charge of variable polarity /1, 2/.

Charge from reference terminal and input terminal are summed in an integrator. The integrator is inside a feedback loop, whose action is to control the polarity of the reference charge so that the integrator output averages

to zero. This occurs when the magnitude of the average reference charge is equal over time to the input charge, hence the name - charge balancing converter. The reference charge is derived by charging a known capacitor to a known (reference) voltage. The polarity of reference voltage is varied. In a conventional voltage input $\Sigma\Delta$ converter, the unknown charge is derived from charging a fixed capacitor to an unknown input voltage, while in the capacitance to digital converter (CDC) realization, the voltage is fixed and the capacitor is variable. Such arrangement provides the high precision and accuracy that are typical for $\Sigma\Delta$ ADCs /3,4/. Modern implementations enable measurement of capacitances in atto Farad (aF) range /4, 5/, with effective noise resolution of 21 bits and corresponding resolution down to 4 aF. They offer measurements of common-mode capacitance up to 17 pF on 4 pF range with 4 fF measurement accuracy. These implementations offer complete sensor solutions, however their application is limited to indication of temperature and humidity dependence problem /6/ of capacitive sensors, while not offering an effective implementation for compensation of these unwanted quantities. In the following work an effective method of temperature compensation of capacitive pressure sensors will be presented.

2.   Setup and measurements

The layout of designed capacitive sensor measurement system is depicted in Figure 1. Capacitive sensor with the CDC AD7746 is shown leftmost. The sensor is connected via interface module to the I²C - USB converter, which is used to interface the sensor to the host PC.
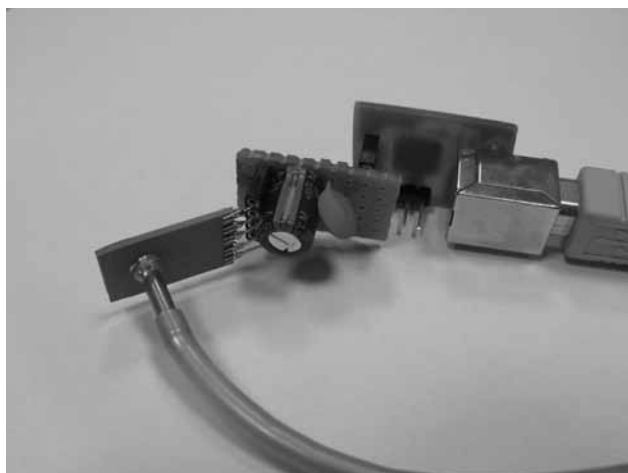

Fig. 1:   General layout of the capacitive sensor evaluation module.

A dedicated electronic interface module was designed. This module enables data transmission and control of CDC AD7746. The module itself is based on a CY8C24794 Programmable System on Chip (PSoC) circuit. The hardware is used to directly map the CDC to the controlling PC. Designed PC software performs the functions of CDC status and data reading. In fact, the controlling software imple-

ments all functions of AD7746: from capacitance channel setup to the temperature sensor channel setup as well as channel excitation, common mode capacitance setting, offset and gain of capacitance measurement channel.

Measurement range optimization was performed in order to get maximal span of CDC measurement range. Measured device, the LTCC capacitive sensor /7/, exhibits negative slope of sensor characteristic. Therefore, the measurement range optimization must be performed at maximal pressure readout with minimal pressure applied and vice versa.

This indicates that the offset compensation must be performed before the gain compensation. Sensor offset response is compensated by setting AD7746 registers CAPDACA and CAPOFFSET. The register value CAPDACA value affects coarse setting of offset response and the CAPOFFSET affects fine setting of sensor response. The procedure of offset setting is comprised of coarse and fine offset setting. Because of negative sensor characteristic slope, the fine offset value is initially set at maximum and the coarse value is altered from its initial zero value in such manner, that the raw sensor readout maintains its maximal value. The setting of CAPDACA register is performed by successive approximation approach, starting at MSB of CAPDACA register. The subsequent bits are tested against raw sensor output. If the sensor output exceeds the maximal sensor readout (FFFF$_{16}$) when corresponding bit is set to 1, then the bit is set to zero and the algorithm advances towards lower bits. After the coarse register was set, the CAPOFFSET register is processed in a similar manner. The result of this algorithm is a maximal sensor response value at applied offset pressure.

After successful optimization of offset value, the gain parameter is set in a similar manner. Minimal sensor response is set with alteration of CAPGAIN register, which actually changes the clock rate of front-end of CDC. The procedure starts with minimal setting of CAPGAIN register. The bits of CAPGAIN register are tested according to described successive approximation algorithm, just the bit-testing criteria is now minimal CDC readout. The result of this algorithm is minimal sensor response at maximal applied pressure. Initial measurements were performed at "Jožef Stefan Institute" /7/. The aim of these measurements was the determination of optimal settings of AD7746 and the tested LTCC sensor. Results of these measurements are depicted in Figure 2. Figure 2 shows the results of sensor characteristic in up and down scan of pressure range. Tested sensor exhibited practically no hysteresis, but the deviation form ideal straight line indicated the necessity for sensor characteristic linearization. The measurements were performed at a room temperature.

Measurements were repeated in HYB d.o.o., Šentjernej. This time, the scan was performed at three different temperatures. Sensor with interface electronic circuit were placed in the temperature chamber and measurement of raw response value was performed at three different temperatures. As the aimed temperature range was set
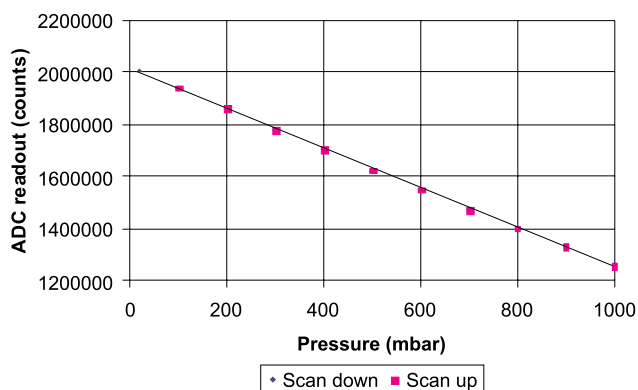
Informacije MIDEM 41(2011)4, str. 272-278

M. Možek, D. Vrtačnik, D. Resnik, B. Pečar, S. Amon:
Compensation And Signal Conditioning Of Capacitive Pressure Sensors.

Fig. 2: Initial pressure sensor measurements.

at 0 °C … 70 °C, the temperature calibration points were selected at 0 °C, 35 °C and 70 °C. The measurements have demonstrated the susceptibility of initial electronic circuit design to electromagnetic interference. Initially it was believed that the long integration setting of AD7746 will solve the problem of 50 Hz hum. As the temperature measurements were performed at temperatures, below room temperature, the chamber compressor switching affected the sensor readout as depicted in Figure 3.
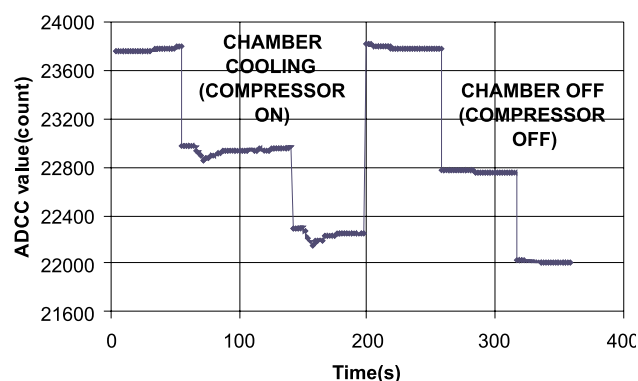

Fig. 3: Sensor readout at lower temperatures.

Figure 3 is showing raw CDC response versus number of samples. The sample rate was set at two samples per second. The left part of Figure 3 is showing disturbed CDC readout when temperature chamber compressor was switched. Pressure was increased from offset to full scale in three increments. The right part of Figure 3 is showing the CDC readout with compressor turned off and again
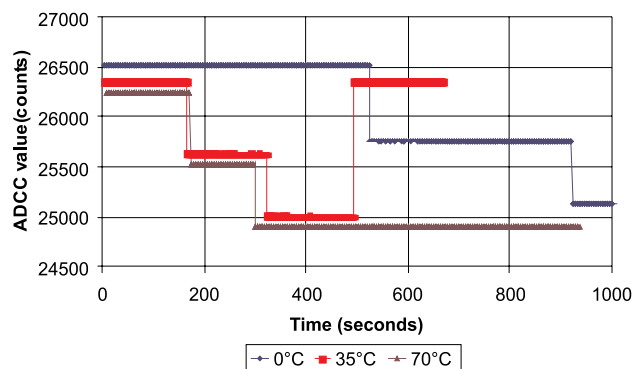

Fig. 4: CDC readout stability.

with three pressure settings, ranging from offset to maximal pressure. As the temperature was elevated above room temperature, the CDC readout diminished, as the compressor is not needed for achievement of higher temperatures. Sensor was fitted with additional shielding (tin foil) and the shielding terminal was grounded in further measurements. Results of raw CDC response stability are shown in Figure 4 at three different temperatures at 0 °C, 35 °C and 70 °C.

Sensor responses were evaluated and stabilized CDC raw response points were obtained at different temperatures. Results of stabilized raw CDC readouts at different temperatures are depicted in Figure 5. At each temperature setting, three pressure points were obtained. Acquired stability results are showing 12 % of sensor response degradation over temperature increase from 0 °C to 35 °C. This turned our attention to more elaborate temperature analysis of sensor properties.
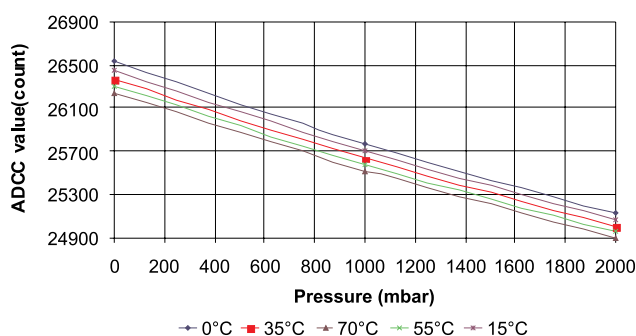

Fig. 5: Stabilized CDC readouts vs. pressure over entire temperature range.

Acquired sensor characteristics were redisplayed as a function of temperature. Resulting data is depicted in Figure 6. This enabled further sensor temperature properties assessment. Analysis from Figure 6 has shown, that tested sensor exhibits a typical pressure span of 1400 counts over 2000 mbar range, which yields approximately an average sensitivity of −0.7 counts/mbar. The temperature coefficient of offset was evaluated as a normalized sensor response over observed temperature range. A large sensor offset temperature coefficient was found at 0.3% FS/°C, which results in total 21% change of sensor offset over temperature range. More encouraging was a low temperature coefficient of sensitivity value, which was estimated at 0.04% FS/°C.
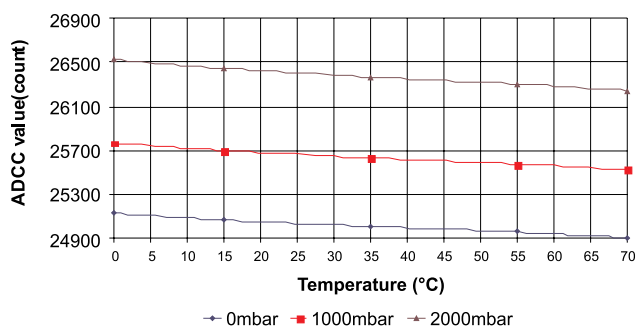

Fig. 6: Stabilized CDC readouts vs. temperature over entire pressure range.

A fairly consistent 3% change in sensitivity was found over temperature calibration range. This indicates the simplicity of sensitivity compensation. On the other hand, a large dependence of sensor offset requires a more complex offset compensation algorithm.

3.   Temperature compensation

As the CDC produces a digital capacitance readout, we focused our work towards digital implementations of temperature compensations. The CDC features ΣΔ approach, the sample rate is limited to several tenths of samples (90 SPS maximum for AD7746), indicating that the increasing complexity of digital processing after acquisition of raw sensor data is not the limiting factor for the entire sensor signal processing.

Temperature compensation of capacitive sensor requires an accurate mathematical description of sensor characteristic in two directions. In case of investigated pressure sensor, the input axes comprise raw pressure and temperature readout and the result is the compensated pressure. Compensation complexity level is depending on sensor nonlinearity of temperature and pressure characteristic. Most adaptable and versatile digital description of sensor characteristic is achieved by Taylor expansion of sensor characteristic. Sensor characteristic expansion can be further segmetned into intervals by writing an expansion around interval ($p_{ocOFFSET}$, $T_{ocOFFSET}$).

$$\Delta p = p_{oc} - p_{ocOFFSET}$$
$$\Delta T = T_{oc} - T_{ocOFFSET} \tag{2}$$

where the raw pressure readout p_{oc} and raw temperature readout T_{oc} are offset with corresponding values $p_{ocOFFSET}$ and $T_{ocOFFSET}$ respectively. Segmentation using (2) further reduces the calibration error.

Taylor series description (3) represents a general approach to sensor characteristic description using segmentation, recommended by IEEE1541.2 standard /8/.

$$p = \sum_{i=0}^{N_P}\sum_{j=0}^{N_T} A_{ij} \cdot \Delta p^i \cdot \Delta T^j \tag{3}$$

Where Δp represents an offset corrected raw readout from capacitive sensor, ΔT represents the offset corrected raw readout from temperature sensor residing on sensor signal conditioner and the N_P and N_T represent the order of Taylor series.

However, such representation requires $N_P \cdot N_T$ calibration points, which is unacceptable. Another major drawback is the use of floating – point calculation coefficients A_{ij} and involution operator. Although algorithms for fast evaluation of (3) were presented /9/, time consuming mathematical operations will reduce the output update rate. On the other hand, the Taylor expansion provides a reasonable start point for initial coefficient relevance. coefficients A_{ij} are obtained by solving a system of linear equations. However, this system is resolved by computing a Vandermonde matrix, which is generally ill conditioned.

In order accommodate abovementioned drawbacks, a two – dimensional Padé approximant, also named Chisholm approximant /10/, is evaluated. This evaluation inherently reduces the number of required calibration points by one.

$$A(p_{oc}, T_{oc}) = \sum_{i=0}^{N_P}\sum_{j=0}^{N_T} a_{ij} \cdot \Delta p^i \cdot \Delta T^j$$
$$B(p_{oc}, T_{oc}) = \sum_{i=0}^{N_P}\sum_{j=0}^{N_T} b_{ij} \cdot \Delta p^i \cdot \Delta T^j$$
$$p(p_{oc}, T_{oc}) = \frac{A(p_{oc}, T_{oc})}{B(p_{oc}, T_{oc})} \quad \text{where} \quad b_{00} = 1 \tag{4}$$

For effective temperature compensation of capacitive sensor signal conditioner a two-dimensional rational polynomial for pressure calculation is used /11/. This type of digital temperature compensation enables correction of nonlinearities up to second order.

$$p = \frac{A_0 + \Delta P + A_1 \cdot \Delta P^2 + A_2 \cdot \Delta T + A_3 \cdot \Delta T^2}{A_4 + A_5 \cdot \Delta T + A_6 \cdot \Delta T^2} \tag{5}$$

Where A_0 through A_6 are calibration coefficients of pressure sensor. Pressure sensor characteristic can be described with inverse proportion of A_4 to sensor sensitivity and the ratio of A_0/A_4 in proportion to sensor offset. Ratio of coefficients A_2 and A_5 are in direct proportion to linear dependence of sensor temperature sensitivity, while the ratio of coefficients A_3 and A_6 represents the quadratic dependence of sensor temperature sensitivity. Value of p corresponds to the normalized pressure output. The value of p lies within interval /0..1/. Value of Δp represents an offset corrected raw readout from capacitive sensor, while the value of ΔT represents the offset corrected raw readout from temperature sensor residing on sensor signal conditioner according to equation (2).

Note that in a given formulations of sensor characteristic description (3) and (4), the actual temperature and capacitance readouts have only indirect significance to final measured quantity p, since the calculation of sensor characteristic description does not depend on actual value of capacitance or temperature.

In case of presented sensor, the pressure dependence of sensor characteristic can be described with linear relationship, while the temperature dependence can be described with quadratic relationship. Measurement resolution was set at 16 bits, maximum obtained resolution of AD7746 for described measurement setup.

The abovementioned observations result in a simplified form of temperature compensation principle for capacitive sensor by setting coefficient A_0 in (2) – the quadratic dependence of capacitive pressure sensor to zero, thus reducing the number of calibration points.

The solution for the unknown coefficients $A_0...A_6$ can be found by solving a system of linear equations, obtained from calibration data, depicted in Figure 6. Seven calibration points are selected and ordered into calibration scenario. Calibration scenario represents a sequence of calibration points, comprised of boundary values, which define the

Informacije MIDEM 41(2011)4, str. 272-278

M. Možek, D. Vrtačnik, D. Resnik, B. Pečar, S. Amon:
Compensation And Signal Conditioning Of Capacitive Pressure Sensors.

pressure and temperature calibration interval. Remaining calibration points are selected at mid – scale of temperature and pressure range, which result in total nine calibration point mesh. The excess two calibration points are used for verification of total calibration error.

4. Results

Software for acquisition, analysis and calibration of capacitive sensors was designed. Table 1 summarizes the evaluation of data depicted in Figure 6. First seven calibration points were used for evaluation of calibration coefficients.

Table 1: Input calibration data.

CP#	P_{CAL}(mbar)	T(°C)	p_{OC}	T_{OC}
1	0	0	26526	16406
2	1000	0	25767	16406
3	2000	0	25123	16406
4	0	35	26366	16524
5	2000	35	25006	16524
6	0	70	26245	16651
7	2000	70	24902	16651
8	1000	35	25630	16524
9	1000	70	25522	16651

Additional test points, which were obtained during the acquisition stage of the calibration process, are summarized in Table 2. The first two test points were a part of acquisition of the calibration process and the remaining points were obtained during temperature scan.

Table 2: Input testpoint data.

TP#	P(mbar)	p_{OC}	T_{OC}	T(°C)
1	1000	25630	16524	35
2	1000	25522	16651	70
3	0	26446	16465	15
4	1000	25698	16465	15
5	2000	25064	16465	15
6	0	26305	16587	55
7	1000	25576	16587	55
8	2000	24954	16587	55

Data was first analyzed using a Taylor expansion for coefficient relevance assessment. This description uses 9 calibration points in order to determine all calibration coefficients. Calibration coefficients were obtained by solving a linear system of equations based on Taylor expansion (3). Resulting calibration coefficients are summarized in Table 3. Taylor expansion coefficients confirm the small nonlinearity (A_{02}) of characterized sensor in pressure direction. Furthermore, results in Table 3 show that linear and quadratic terms are dominant for successful sensor compensation, while the small cross – products between pressure and temperature direction indicate, that sensor characteristic evaluation can be simplified.

Table 3: Calculated calibration coefficients of Taylor expansion.

A_{00}	1772.47	A_{12}	7.18E-07
A_{01}	-1.35	A_{20}	1.94E-03
A_{02}	-1.40E-05	A_{21}	1.72E-07
A_{10}	-3.49	A_{22}	-6.66E-10
A_{11}	-8.71E-05		

Evaluation of a Taylor expansion (2) using coefficients listed in Table 3 was performed. Equation (2) was evaluated at testpoints in Table 2. Results are shown in Table 4, which lists the calibration error ε.

$$\varepsilon = \left| \frac{P_{CAL} - P_{EVAL}}{FS} \right| \cdot 100\%$$

(6)

Where P_{CAL} represents calibration pressure point, P_{EVAL}, evaluation pressure and FS the output pressure span. Results summarized in Table 4 are in fair agreement with calibration pressure points. A 0.5% discrepancy was found at the endpoint of temperature calibration range at testpoint 8 (*T=70°C*).

Table 4: Calculated calibration coefficients of Taylor expansion.

T_{OC}	p_{OC}	P_{CAL}	P_{EVAL}	ε(%)
16465	25064	2000	1995.69	-0.22
16465	25698	1000	993.60	-0.32
16465	26446	0	-6.92	-0.35
16587	24954	2000	1995.48	-0.23
16587	25576	1000	992.37	-0.38
16587	26305	0	-9.36	-0.47

Simplification is performed by introduction of Chisholm approximant for sensor characteristic description. Chisholm approximant of degree (1,2) would require 11 calibration coefficients.

This lead to evaluation of a linear Padé (1,1) approximant, which requires 7 coefficients for evaluation. Calibration dataset was taken from first seven calibration points in Table 1. Resulting coefficients are summarized in Table 5.

Table 5: Resulting Padé (1, 1) calibration coefficients.

a_{00}	1666.67	b_{00}	1
a_{01}	-1.47	b_{01}	1.68E-03
a_{10}	-0.60	b_{10}	5.48E-04
a_{11}	-3.51E-03	b_{11}	-6.28E-07

Equation (4) was evaluated at testpoints in Table 2. Results are shown in Table 6, which lists the calibration error ε according to equation (4).

Results in Table 6 are in fair agreement with calibration pressure points. A rather large 1.5% discrepancy occurs at the endpoint of temperature calibration range at testpoint 2 (*T=70°C*).

Table 6: Evaluation error at testpoint data.

TP#	P_{CAL} (mbar)	P_{EVAL} (mbar)	$|\varepsilon(\%)|$
1	1000	1000	0.0
2	1000	1030.7	1.53
3	0	-8.7	0.43
4	1000	972.7	1.36
5	2000	1995.84	0.20
6	0	−5.32	0.26
7	1000	1011.6	0.58
8	2000	1996.55	0.17

In order to further improve compensation accuracy, a Padé (2,2) approximant was analyzed. A full evaluation of Padé (2,2) approximant would require a set of 17 calibration points, which is unacceptable for mass production of sensors. The original evaluation was therefore normalized with coefficient $4/A_4$ factor and cross products terms of temperature and pressure were neglected. In order to minimize computational errors, coefficients were weighed according to:

$$p = \frac{2^2 \cdot \Delta P + 2^{-24} \cdot A_0 \cdot \Delta P^2 + A_1 + 2^{-9} \cdot A_2 \cdot \Delta T + 2^{-18} \cdot A_3 \cdot \Delta T^2}{A_4 + 2^{-9} \cdot A_5 \cdot \Delta T + 2^{-18} \cdot A_6 \cdot \Delta T^2} \tag{7}$$

Evaluation of system of linear equations based on equation (4) yields the calibration coefficients summarized in Table 2.

Table 7: Resulting calibration coefficients.

A_0	A_1	A_2	A_3	A_4	A_5	A_6
-8192	-5057	4999	-1391	-12931	2147	-1202

Equation (4) was evaluated at testpoints in Table 3. Results are shown in Table 8. A maximum 0.4% deviation from measured data was found at 0 mbar both at 0 °C and 70 °C, while the compensation remains well in typical industrial sensor applications (0.5% admissible temperature error over entire temperature calibration range).

Table 8: Evaluation error at testpoint data.

TP#	P_{CAL} (mbar)	P_{EVAL} (mbar)	$|\varepsilon(\%)|$
1	1000	1006	0.3
2	1000	1003	0.15
3	0	-8	0.4
4	1000	998	0.1
5	2000	1997	0.15
6	0	−7	0.35
7	1000	999	0.05
8	2000	1996	0.2

4.   Conclusions

Implementation of a digital temperature compensation method, developed for piezoresistive pressure sensors, to the field of capacitive sensors was presented. Possibilities for the compensation of sensor parameters such as sensor nonlinearity and temperature sensitivity were analyzed. In order to achieve effective compensation and linearization, different digital descriptions of sensor characteristic were investigated and reported, such as two-dimensional rational polynomial description derived from Padé approximations. Evaluation results of sensor response were compared against reference pressure source and most effective digital temperature compensation was proposed. Proposed digital compensation yields maximum 0.4% FS error on a compensation range $0 - 70$ °C and enables integer arithmetic, thus making proposed approach appropriate for use in modern sensor signal conditioning integrated circuits.

References

/1/   S. R. Norsworthy, R. Schreier, G. C. Temes, "Delta-Sigma Data Converters" IEEE Press, 1997, Wiley-IEEE Press, ISBN: 978-0780310452.

/2/   J. C. Candy, G. C. Temes, "Oversampling Delta-Sigma data converters", IEEE Press, Publisher: Wiley-IEEE Press, 2008, ISBN: 978-0879422851.

/3/   O'Dowd, J. Callanan, A. Banarie, G. Company-Bosch, E "Capacitive sensor interfacing using sigma-delta techniques" Sensors, 2005 IEEE, pp.-951-954, ISBN: 0-7803-9056-3. Digital Object Identifier: 10.1109/ICSENS.2005.1597858

/4/   Markus Bingesser, Teddy Loeliger, Werner Hinn, Johann Hauer, Stefan Mödl, Robert Dorn, Matthias Völker "Low-noise sigma-delta capacitance-to-digital converter for Sub-pF capacitive sensors with integrated dielectric loss measurement" Proceedings of the conference on Design, automation and test in Europe, Munich, Germany, 2008, pp. 868-872.

/5/   Analog Devices AD7746 Evaluation Board - EVAL-AD7746EB, Revision 0, May 2005. Available on: http://www.analog.com/static/imported-files/eval_boards/252730993EVAL_AD7746EB_0.pdf

/6/   Susan Pratt «Environmental Compensation on the AD7142: The Effects of Temperature and Humidity on Capacitance Sensors» Analog Devices Application Note AN-829, 2005. Available on: http://www.analog.com/static/imported-files/application_notes/577315308337353595958633AN829_0.pdf

/7/   Belavič Darko, Santo-Zarnik Marina, Hrovat Marko, Maček Srečo, Kosec, Marija. «Temperature behaviour of capacitive pressure sensor fabricated with LTCC technology» Inf. MIDEM, 2009, vol. 38, no. 3, pp. 191-196.

/8/   IEEE Std. 1451.2 D3.05-Aug1997 *"IEEE standard for a smart transducer interface for sensors and actuators – Transducer to microprocessor communication protocols and transducer electronic data sheet (TEDS) formats"* Institute of Electrical and Electronics Engineers, September 1997.

/9/   MOŽEK, Matej, VRTAČNIK, Danilo, RESNIK, Drago, ALJANČIČ, Uroš, AMON, Slavko. *Fast algorithm for calculation of measured quantity in smart measurement systems*, 39th International Conference on Microelectronics, Devices and Materials and the Workshop on Embedded Systems, October 01. – 03. 2003, Ptuj, Slovenia. Proceedings. Ljubljana: MIDEM - Society for Microelectronics, Electronic Components and Materials, 2003, pp. 111-116.

/10/   Baker, George A. Graves-Morris, P. R., Padé approximants. #Part #1, Basic theory, Reading (Mass.) /etc./ : Addison-Wesley, 1981, (Encyclopedia of mathematics and its applications ; #vol. #13).

/11/   ZMD31020 Advanced Differential Sensor Signal Conditioner Functional Description Rev. 0.75, (2002) ZMD AG.

dr. Matej Možek, univ. dipl. inž. el.
matej.mozek@fe.uni-lj.si, tel.: 01 4768 380
dr. Danilo Vrtačnik, univ. dipl. inž. el.
danilo.vrtacnik@fe.uni-lj.si, tel.: 01 4768 303
dr. Drago Resnik, univ. dipl. inž. el.
drago.resnik@fe.uni-lj.si, tel.: 01 4768 303
Borut Pečar, univ. dipl. inž. el.
borut.pecar@fe.uni-lj.si, tel.: 01 4768 303

prof. dr. Slavko Amon, univ. dipl. inž. fiz.
slavko.amon@fe.uni-lj.si, tel.: 01 4768 352

LMSE, FE-UL, Tržaška 25, SI-1000 Ljubljana